Geol. Mag. **156** (*5*), *2019, pp. 759–771* © *Cambridge University Press 2018*
doi:10.1017/S001675681800002X

Carbon-isotope stratigraphy of the uppermost Cambrian in eastern Laurentia: implications for global correlation

KAREM AZMY*

Department of Earth Sciences, Memorial University of Newfoundland, St. John's, Newfoundland A1B 3X5, Canada

(*Received* 15 September 2017; *accepted* 4 January 2018; *first published online* 12 February 2018)

Abstract – The $\delta^{13}C$ profile from an interval of the Martin Point section in western Newfoundland (Canada) spans the upper Furongian (uppermost Cambrian). The interval (~90 m) is a part of the Green Point Formation of the Cow Head Group and consists of the Martin Point (lower) and the Broom Point (upper) members. It is formed of slope marine carbonates alternating with shales (rhythmites) and conglomeratic interbeds. The preservation of the investigated micritic carbonates was meticulously evaluated by multiple petrographic and geochemical screening tools. The $\delta^{13}C$ and $\delta^{18}O$ values (-0.5 ± 0.8 ‰VPDB and -7.1 ± 0.3 ‰VPDB, respectively) exhibit insignificant correlation ($R^2 = 0.002$) and similarly the correlation of $\delta^{13}C$ values with their Sr and Mn counterparts, which supports the preservation of at least near-primary $\delta^{13}C$ signatures that can be utilized to construct a reliable high-resolution carbon-isotope profile for global correlations.

The $\delta^{13}C$ profile exhibits two main negative excursions, a lower broad excursion (~3 ‰) that reaches its maximum at ~70 m below the Martin Point / Broom Point members boundary and an upper narrow excursion (~2.5 ‰) immediately below the same boundary. The lower excursion can be correlated with the global latest Furongian HERB event (TOCE), which is also recognized in the C-isotope profile of the GSSP boundary section at Green Point whereas the upper excursion matches with that of the Cambrian–Ordovician boundary in the same section. The peak of the HERB $\delta^{13}C$ excursion is correlated with positive shifts on the Th/U and Ni profiles (redox and productivity proxies).

Keywords: Furongian (latest Cambrian), HERB event, high-resolution $\delta^{13}C$ chemostratigraphy, palaeoenvironmental changes, slope carbonates, eastern Laurentia (NL, Canada)

1. Introduction

Primary stable isotope signatures retained in Phanerozoic carbonates (e.g. Veizer *et al.* 1999) have become increasingly used as a potential tool for refining global stratigraphic correlations, particularly those of the Early Palaeozoic that have poor biostratigraphic resolution or biostratigraphic correlation problems. Primary/near-primary carbon-isotope variations associated with eustasy allow the construction of reliable profiles for correlating sedimentary sequences of different depositional settings within the same basin and from different palaeocontinents (e.g. Jing *et al.* 2008; Miller *et al.* 2011, 2014; Azomani *et al.* 2013; Terfelt, Eriksson & Schmitz, 2014). The eustatic changes along the eastern Laurentian passive margin during the latest Cambrian influenced the redox conditions of the depositional environment and accordingly primary organic productivity along with the C-isotope compositions of marine carbonates (Landing, 2007, 2012; Landing, Westrop & Miller, 2010; Miller *et al.* 2011, 2014; Azmy *et al.* 2014, 2015; Terfelt, Eriksson & Stouge, 2014).

The evaluation of preservation of the $\delta^{13}C$ signatures, in earlier studies, was mainly based on their insignificant correlation with their $\delta^{18}O$ counterparts, but elemental proxies were rarely discussed. Therefore, the main objectives of the current study are to evaluate in detail the petrographic and geochemical preservation of the carbonates of the Martin Point section (western Newfoundland, Canada) that spans the uppermost (Furongian) Cambrian and to reconstruct a reliable primary C-isotope profile that allows recognition of the stratigraphic levels of the HERB event (Hellnmaria – Red Tops Boundary; also called TOCE (Top Of Cambrian Excursion)). This will also enhance the global correlation of the uppermost Cambrian sequences on eastern Laurentia and beyond.

2. Geological setting

Palaeozoic sedimentary rocks of western Newfoundland (Fig. 1) were deposited on the eastern (palaeo-southern) Laurentian margin. The Laurentian plate developed by active rifting around 570–550 Ma (e.g. Cawood, McCausland & Dunning, 2001; Hibbard, Van Staal & Rankin, 2007), and a pre-platform shelf formed and was eventually covered by clastic sediments (James *et al.* 1989). A major transgression flooded the Laurentian platform margin and resulted in the accumulation of thick carbonate deposits,

*Author for correspondence: kazmy@mun.ca

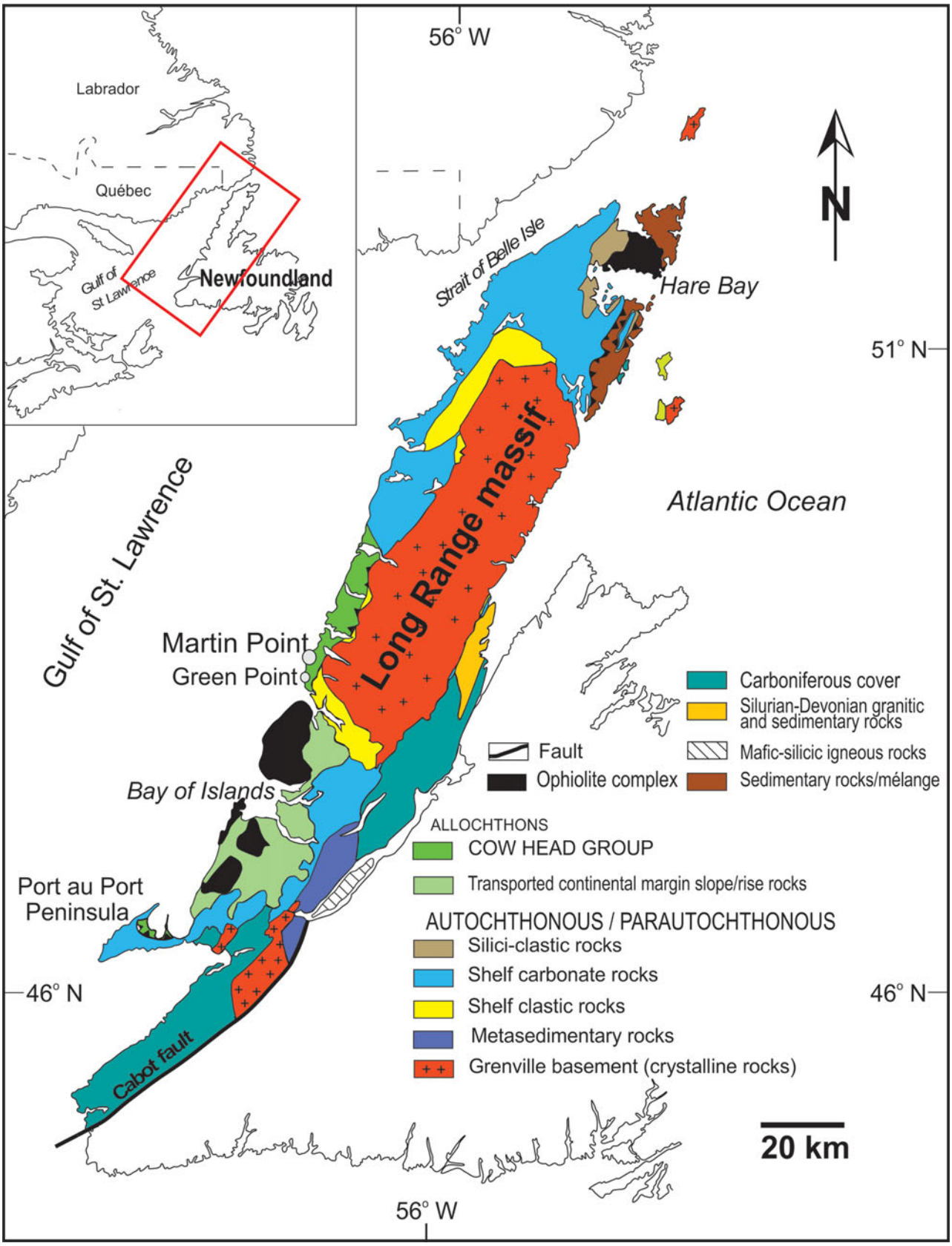

Figure 1. (Colour online) Map of the study area showing the surface geology and location of the Martin Point section (49° 40′ 51″ N; 57° 57′ 36″ W) in western Newfoundland, Canada (modified from Cooper, Nowlan & Williams, 2001).

https://doi.org/10.1017/S001675681800002X Published online by Cambridge University Press

particularly during the Late Cambrian (Wilson *et al.* 1992; Landing, 2007, 2012; Lavoie *et al.* 2012).

3. Stratigraphy

3.a. Lithostratigraphy

The lithostratigraphy of the investigated interval of the Martin Point section, which is part of the Green Point Formation of the Cow Head Group (Fig. 2), has been studied and discussed in detail by James & Stevens (1986), and is therefore only summarized here. It consists of the uppermost part of the Cambrian Martin Point Member and lowermost part of the overlying Ordovician Broom Point Member, which are generally composed of rhythmites of dark-grey to black fissile shale alternating with thin (~1 cm-thick) interbeds of ribbon limestone (micritic to near-micritic) that are very fine-grained (James & Stevens, 1986). Siltstone interbeds (up to 1 cm thick) may co-occur with shale, and the limestone interbeds vary from isolated and thin to up to 20 cm thick. Conglomerate beds, deposited by turbidites (James & Stevens, 1986), occur in both members and contain blocks of shallow water carbonates that were transported into deep-water facies along the slope of the Laurentian margin (James & Stevens, 1986). The overlying Lower and Middle Ordovician strata are composed of shale with occasional limestone horizons. These distal shales are mostly red, indicating accumulation under oxidizing conditions above a postulated oxygen minimum layer or continental red muds that were shed in the basin and rapidly accumulated (James & Stevens, 1986).

3.b. Biostratigraphy

The investigated interval spans, from bottom to top, the *Proconodontus muelleri, Eoconodontus notchpeakensis, Cordylodus proavus* and *Cordylodus caboti* conodont zones (Furongian, uppermost Cambrian) (James & Stevens, 1986; Barnes, 1988; Miller *et al.* 2011; Stouge, Bagnoli & Azmy, 2016).

Rooted benthic graptolites appear in the lower part of the succession and extend upwards, where planktonic graptolites (*Rhabdinopora flabelliformis* subspecies) appear just above the Cambrian–Ordovician boundary. The top of the Broom Point Member contains a prolific assemblage of graptolites of early Tremadocian age (James & Stevens, 1986; Williams & Stevens, 1991).

4. Material and methodology

Sixty-four closely spaced samples (sampling intervals as small as 10 cm; Appendix and Fig. 2) were collected from the Martin Point section (49° 40′ 51″ N, 57° 57′ 36″ W), western Newfoundland (Fig. 1). Samples were taken from the most micritic lime mudstones to avoid allochthonous clasts. Thin-sections of samples were petrographically examined with a polarizing microscope and stained with Alizarin Red – S and potassium ferricyanide solutions (Dickson, 1966). Cathodoluminescence (CL) observations were performed using a Technosyn 8200 MKII cold cathode instrument operated at 8 kV accelerating voltage and 0.7 mA current.

A mirror-image slab of each thin section was also prepared and polished for microsampling. These polished slabs were washed with deionized water and dried overnight at 50° C prior to isolating the finest-grained lime mudstone free of secondary cements and other contaminants. Due to the possible heterogeneity in geochemical composition of texturally distinct carbonate phases in whole-rock samples, and in order to avoid silicate-rich and secondary carbonate cements and veins, microsamples were drilled from the finest-grained micritic material under a binocular microscope. Approximately 10 mg of carbonate was microsampled from the cleaned slabs using a low-speed microdrill.

For C- and O-isotope analyses, about 220 μg of powder sample was reacted in an inert atmosphere with ultrapure concentrated (100 %) orthophosphoric acid at 70 °C in a Thermo Finnigan GasBench II. The liberated CO_2 was automatically delivered to a Thermo Finnigan DELTA V plus isotope ratio mass spectrometer in a stream of helium, where the gas was ionized and measured for isotope ratios. Uncertainties of better than 0.1 ‰ (2σ) for the analyses were determined by repeated measurements of NBS-19 ($\delta^{18}O = -2.20$ ‰ and $\delta^{13}C = +1.95$ ‰ vs VPDB) and L-SVECS ($\delta^{18}O = -26.64$ ‰ and $\delta^{13}C = -46.48$ ‰ vs VPDB).

For elemental analyses, a subset of sample powder (~10 mg each) was digested in 2 % (v/v) HNO_3 and analysed for major and trace elements using an Elan DRC II ICP-MS (inductively coupled plasma mass spectrometer) (Perkin Elmer SCIEX) at Memorial University of Newfoundland. The relative uncertainties of these measurements are less than 5 %, and results are normalized to a 100 % carbonate basis (e.g. Azmy *et al.* 2014).

5. Results

Petrographic examinations indicate that the sampled carbonates are dominantly lime mudstones, which have retained micritic to near-micritic (<4 to 10 μm) texture and appear dull under cathodoluminescence (Fig. 3a, b).

The geochemical attributes of the investigated Martin Point carbonates are described in detail in the Appendix, and their statistics are summarized in Table 1. Their mean Sr (324 ± 192 ppm) is slightly higher than their counterparts of the GSSP (global boundary stratotype section and point) carbonates at Green Point (Table 1; Azmy *et al.* 2014) although their Mn content (360 ± 160 ppm) is slightly lower (Table 1) and the Sr and Mn values are poorly correlated ($R^2 = 0.1$). The Sr contents are also poorly correlated with their $\delta^{13}C$ counterparts (Fig. 4a;

https://doi.org/10.1017/S001675681800002X Published online by Cambridge University Press

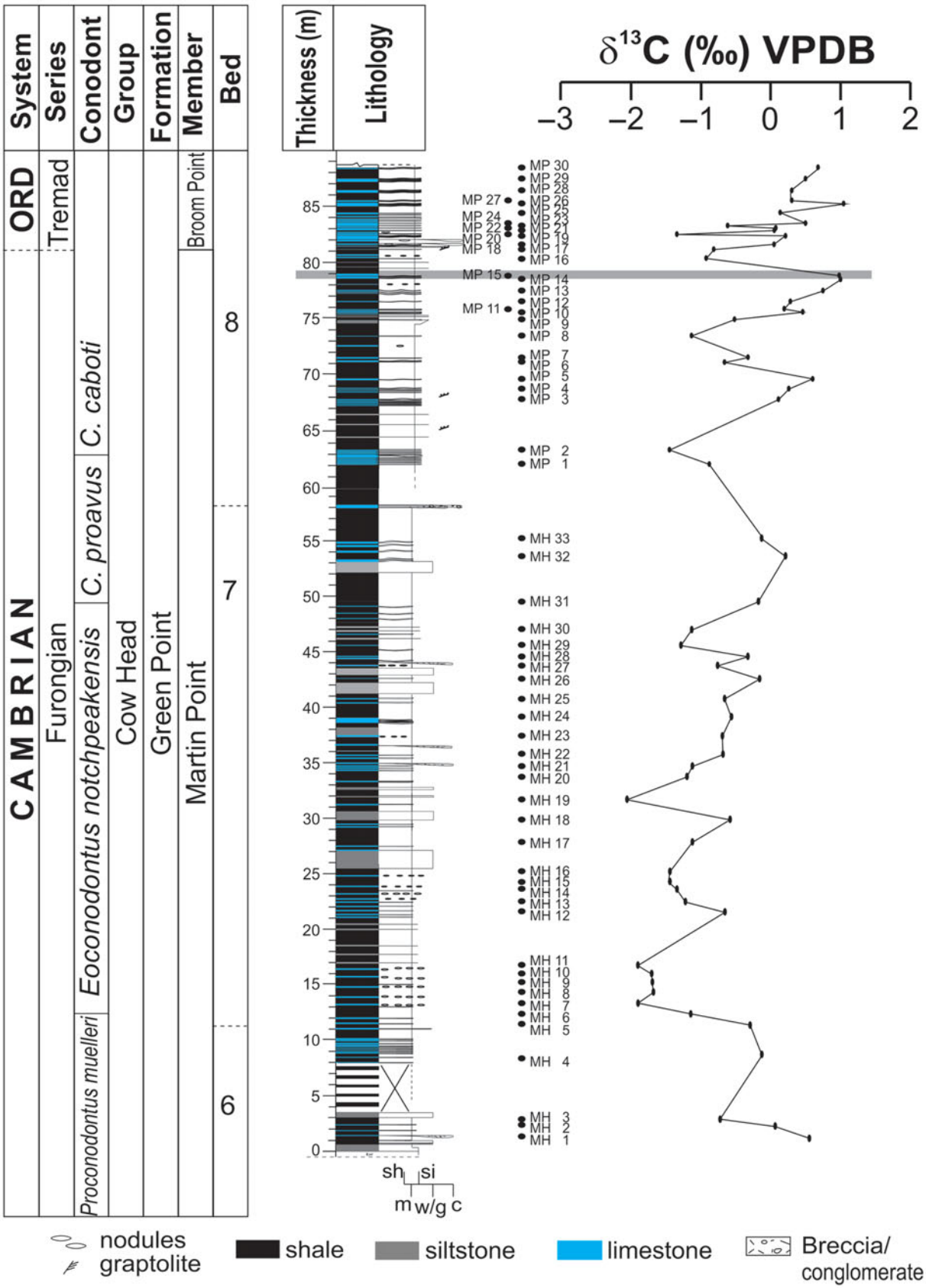

Figure 2. (Colour online) Stratigraphic framework of the investigated Martin Point section in western Newfoundland, Canada, showing bed number and detailed measured positions of investigated samples and conodont zonation scheme (Barnes, 1988). The solid grey line marks the approximate level correlated with the geochemical anomaly documented by Azmy *et al*. (2014, 2015), which revealed distinct geochemical changes across the Cambrian–Ordovician boundary in the GSSP section.

https://doi.org/10.1017/S001675681800002X Published online by Cambridge University Press

Table 1. Statistics of the geochemical compositions of the investigated Martin Point carbonates.The Green Point data (from Azmy *et al.* 2014) represent the Cambrian–Ordovician boundary interval (GSSP)

	$CaCO_3$ (%)	$MgCO_3$ (%)	Mn (ppm)	Sr (ppm)	$\delta^{13}C$ (‰VPDB)	$\delta^{18}O$ (‰VPDB)
Martin Point section						
n	25	25	25	25	63	63
average	98.4	1.6	360	324	– 0.5	– 7.1
stdev	0.7	0.7	160	192	0.8	0.3
max	99.0	3.7	649	980	1.0	– 6.4
min	96.3	1.0	142	152	– 2.1	– 7.8
Green Point section (Cambrian–Ordovician GSSP)						
n	62	62	62	62	84	84
average	97.4	2.6	392	271	– 0.9	– 7.4
stdev	6.4	6.4	220	74	1.4	0.5
max	99.1	38.0	1054	510	1.7	– 5.5
min	62.0	0.9	90	175	– 4.7	– 8.7

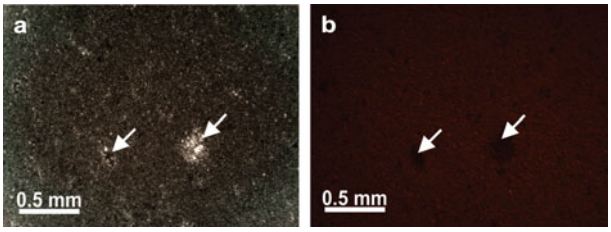

Figure 3. (Colour online) Photomicrographs of the investigated carbonates showing (a) micritic lime mudstones from Martin Point section micrites (sample MP28) and (b) CL image of (a). Arrows point at late cement in microvugs that appears non-luminescent.

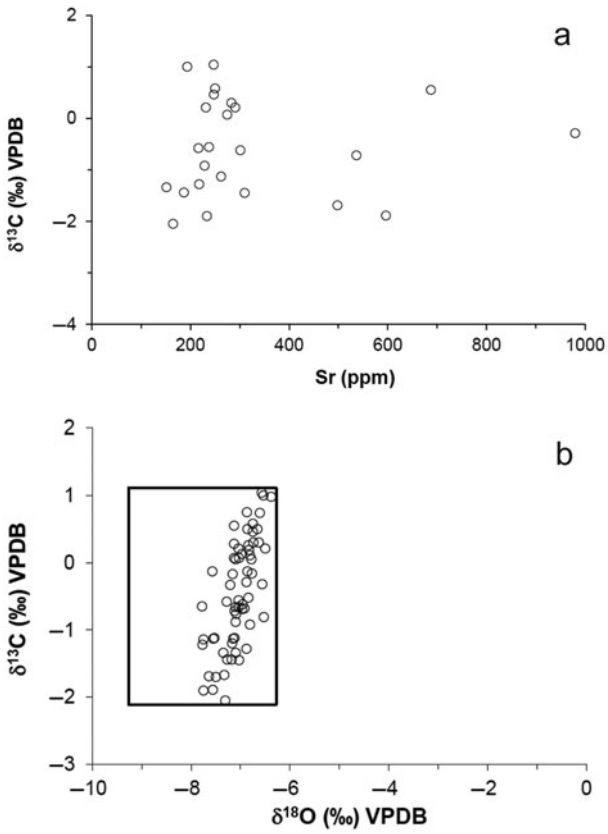

Figure 4. Scatter diagrams showing correlations of (a) Sr with $\delta^{13}C$ and (b) $\delta^{18}O$ with $\delta^{13}C$ for the micritic lime mudstones from the Martin Point section. The rectangle in (b) shows the composition of well-preserved uppermost Cambrian and lowermost Ordovician marine carbonates (Veizer *et al.* 1999).

$R^2 = 0.0006$) and similarly the Mn contents ($R^2 = 0.03$; Appendix). The mean $\delta^{13}C$ and $\delta^{18}O$ values of the Martin Point carbonates (–0.5 ± 0.8 and –7.1 ± 0.3 ‰ VPDB, respectively; Table 1) are comparable to their counterparts of the GSSP section in Green Point although they might be slightly enriched (Table 1; Azmy *et al.* 2014) and they fall within the documented range of Upper Cambrian well-preserved marine carbonates (Veizer *et al.* 1999; Fig. 4b). The $\delta^{13}C$ profile exhibits a broad negative excursion, consisting of subpeaks, that reaches its most negative value at the base of bed 7 and the base of the *E. notchpeakensis* Zone (Fig. 5). This peak negative value correlates with distinct shifts on the Th/U and Ni profiles (Fig. 5) that are reliable redox and bioproductivity proxies (e.g. Wignall & Twitchett, 1996; Śliwiński, Whalen & Day, 2010). The Th/U values range from 0.1 to 5.1 (1.1 ± 1.3; Appendix) and those of Ni from 1.4 to 8.5 ppm (3.5 ± 1.8 ppm; Appendix). Both of these proxies have insignificant correlation with their Sr counterparts ($R^2 \leq 0.03$). There is also an upper negative $\delta^{13}C$ excursion that consists of sharp subpeaks and correlates with the Cambrian–Ordovician Boundary.

6. Discussion

Carbon-isotope chemostratigraphy is mainly based on the distinctive variations in the $\delta^{13}C_{carb}$ profile, which may reflect environmental and/or diagenetic perturbations (e.g. Veizer *et al.* 1999; Halverson *et al.* 2005). In ancient sediments, particularly those of the Palaeozoic, it is almost impossible for those sediments to remain entirely unaltered by diagenetic fluids through their burial history. However, the degree of alteration varies depending on the water/rock interaction ratio and the strength of reset of the retained proxy signal (Veizer, 1983; Banner & Hanson, 1990). Thus, restricted diagenesis at near-closed system may not significantly alter some of the proxies and they may provide near-primary signatures that can be utilized to reconstruct the depositional marine settings. Therefore, evaluation of the degree of preservation of the retained (primary or near-primary) isotopic and elemental geochemical signatures is a cornerstone for the reconstruction of a

https://doi.org/10.1017/S001675681800002X Published online by Cambridge University Press

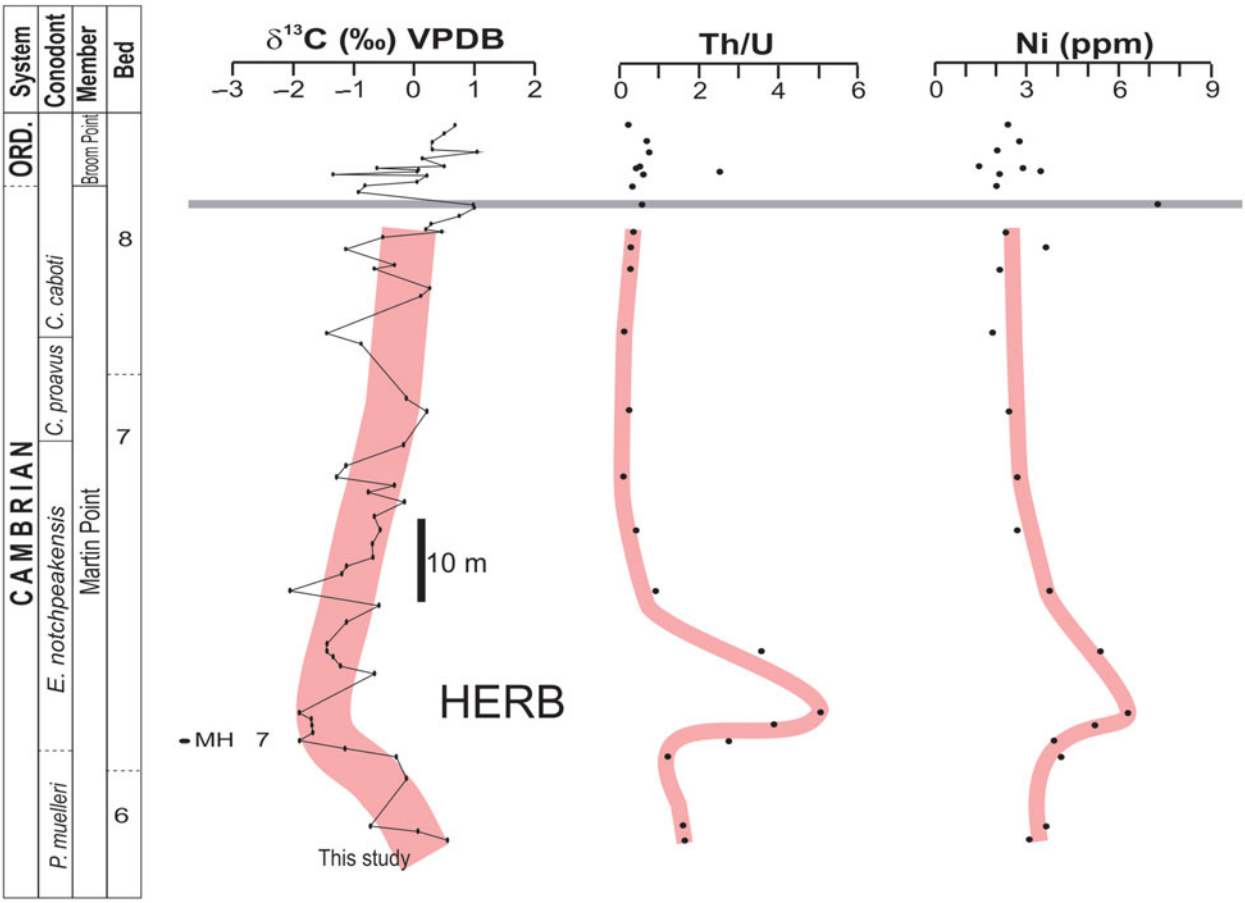

Figure 5. (Colour online) Carbon-isotope, Th/U and Ni profiles spanning the uppermost Cambrian and lowermost Ordovician lime mudstones at Martin Point. The red lines show the general first-order trends of the HERB geochemical profiles of the investigated section at Martin Point. The solid grey line as in Figure 2.

reliable C-isotope profile that can be utilized for high-resolution chemostratigraphic correlations within the same sedimentary basin and also on a global basis.

6.a. Evaluation of sample preservation

The investigated carbonates were examined by multiscreening petrographic and geochemical techniques to evaluate their degree of preservation. The examined interval of the Green Point Formation at Martin Point section spans the Late Cambrian to Early Ordovician and is dominated by lime mudstones that show insignificant recrystallization (Fig. 3a). They retained original sedimentary fabrics and a micritic to near-micritic grain size, thus suggesting a high degree of textural preservation. They also exhibit dull luminescence under a cathodoluminoscope (Fig. 3b) compared with the nearly non-luminescent late cement in microvugs likely due to enrichment of Fe in those cements. Luminescence in carbonates is mainly activated by high concentrations of Mn and quenched by high concentrations of Fe (Machel & Burton, 1991). Dull luminescence, in many cases, indicates relative preservation of primary geochemical signatures although diagenetic carbonates, such as late cements, might still exhibit no luminescence due to high Fe content (Rush & Chafetz, 1990). Therefore, cathodoluminescence should be taken with caution and has to be complemented by additional screening tests (Brand *et al.* 2011).

Diagenetic alteration of carbonates leads to depletion in Sr content and $\delta^{18}O$ values but enrichment in Mn (Veizer, 1983). In an oxic shallow-water environment, the ocean water has low Mn concentrations, but the deeper water of the slope settings (dysoxic or less oxic) is expected to have at least slightly higher Mn. Microbial lime mudstones have been documented in Palaeozoic slope carbonates at depths down to 300 m (e.g. Della Porta *et al.* 2003; Bahamonde, Merino-Tomé & Heredia, 2007). If so, the investigated Martin Point lime mudstones might have had contributions from carbonates that precipitated *in situ* through microbial mediation (cf. George, 1999; Della Porta *et al.* 2003; Bahamonde, Merino-Tomé & Heredia, 2007; Bartley *et al.* 2015) under dysoxic conditions where Mn^{2+} is more available in the seawater and they may therefore have incorporated higher Mn contents (360 ± 160 ppm; Table 1) than those of shallow water environment (≤ 100 ppm; Veizer, 1983). This suggests that their enriched Mn contents are not entirely caused by diagenesis, which agrees with their relatively high Sr contents (up to 980 ppm; Table 1) and with the

https://doi.org/10.1017/S001675681800002X Published online by Cambridge University Press

consistent clean lime mudstone interbeds that lack clastic inclusions (cf. James & Stevens, 1986; Coniglio & James, 1990; Li *et al.* 2006). Also, the Mn contents of the investigated carbonates still have very poor correlation with their $\delta^{13}C$ values ($R^2 = 0.03$; Appendix), which argues against significant alteration of the $\delta^{13}C$ signatures.

On the other hand, the Sr contents of the Martin Point carbonates exhibit insignificant correlation ($R^2 = 0.0002$; Fig. 4a) with their $\delta^{13}C$ counterparts (e.g. Derry, Kaufman & Jacobsen, 1992; Veizer *et al.* 1999; Halverson *et al.* 2005), which supports the preservation of at least near-primary $\delta^{13}C$ values. Also, the poor correlation between the Sr and the $\delta^{18}O$ values ($R^2 = 0.02$; Appendix) suggests that the reset of the $\delta^{18}O$ signatures was restricted, which is consistent with the fact that the isotopic composition of the investigated carbonates falls within that documented for the best-preserved marine carbonates of the same age (Fig. 4b; Veizer *et al.* 1999). This is because the impact of diagenesis on the $\delta^{13}C$ signatures of carbonates is relatively less than that on their $\delta^{18}O$ counterparts since the diagenetic fluids, in many cases, do not contain enough CO_2 to reset the C-isotope composition, which leads to the preservation of near-primary $\delta^{13}C$ signatures of the ancient carbonates. Therefore, the reset of the $\delta^{13}C$ signature requires a high water/rock interaction ratio and is associated with significant recrystallization and increase in crystal size (aggrading neomorphism), which is inconsistent with the micritic to near-micritic grain size of the investigated Martin Point lime mudstones. By contrast, the diagenetic fluids are basically water and their O-isotope composition certainly resets the $\delta^{18}O$ of carbonates quickly at variable degrees depending on the water/rock interaction ratio, and,thus the preservation of primary/near-primary $\delta^{18}O$ signatures in marine lime mudstones is rare compared to their $\delta^{13}C$ counterparts. This may suggest that the poor correlation of Sr, and also Mn ($R^2 = 0.008$; Appendix), with the $\delta^{18}O$ values has to be treated with caution.

Although Fe is enriched with progressive diagenesis like Mn (Veizer, 1983), the possible contamination from hidden bacterial microrhombic pyrite during microsampling, particularly in carbonates associated with sealevel rise and increasing reducing conditions, makes it an unreliable proxy for the evaluation of degree of geochemical preservation.

Alteration of organic matter, which is associated with recrystallization of carbonates, may deplete the primary $\delta^{13}C$ signatures of carbonates. If, for argument's sake, the organic content was high in sediments during deposition and organic remineralization influenced the $\delta^{13}C$ of those carbonates during diagenesis, the effect would be consistent throughout the C-isotope profile and the shifts would be irregular and randomly spread rather than distinct excursions correlated specifically with the Cambrian–Ordovician boundary and with the base of the *E. notchpeakensis* zone (HERB event; Buggisch, Keller & Lehnert, 2003; Miller *et al.* 2011, 2014). No diagenetic model or system has been known so far to cause excursions in the $\delta^{13}C$ profiles of carbonate sections from different palaeocontinents (Buggisch, Keller & Lehnert, 2003; Miller *et al.* 2011, 2014) at the exact stratigraphic level.

In summary, the petrographic evidence of insignificant recrystallization but preservation of sedimentary fabric (cf. Banner & Hanson, 1990), the insignificant correlation between $\delta^{13}C$ and Sr values, the consistency of $\delta^{13}C$ values in closely spaced stratigraphic samples (Appendix) and the similarities between the mean $\delta^{13}C$ value of the Martin Point carbonates and that of the equivalent Cambrian–Ordovician GSSP boundary section counterparts (Table 1) support the preservation of their primary geochemical signatures and suggest that the variations in the $\delta^{13}C$ compositions of the Martin Point carbonates reflect their primary depositional conditions and can be reliably utilized for high-resolution chemostratigraphic correlations (cf. Azmy *et al.* 2001, 2006, 2014; Halverson *et al.* 2005).

6.b. Environmental changes

Changes in sealevel influence oxygen levels in water column and accordingly the oxidation state of redox-sensitive elements. This selectively controls their solubility in seawater and also their degree of enrichment in marine sediments (e.g. Wignall & Twitchett, 1996; Arnaboldi & Meyers, 2007, Wignall *et al.* 2007). In oxidizing environments, uranium ions maintain the higher oxidation state (U^{6+}) and form uranyl carbonate, which is soluble in water, whereas in reducing conditions they retain the lower oxidation state (U^{4+}) and form the insoluble uranous fluoride which is trapped into marine carbonates (Wignall & Twitchett, 1996). Unlike U, Th is not affected by redox conditions in the water column and occurs permanently in the insoluble Th^{4+} state. Thus, sediments of anoxic environments are richer in uranium and have lower Th/U than those of oxic environments. Therefore, the Th/U ratio has been used as a proxy for environmental redox conditions, with ratios <2 in anoxic marine sediments and >2 in oxic sediments of open basins (cf. Wignall & Twitchett, 1996). The insignificant correlation ($R^2 \leq 0.03$) of the Th/U values with their Sr counterparts argues against their impact by diagenesis and suggests that they are at least near-primary signatures since Sr is known to be consistently depleted by diagenesis (Veizer, 1983).

The Th/U values of the Furgonian Martin Point Formation carbonates are generally <2 but they sharply increase to reach ~ 5 near the bottom of Bed 7 before they drop quickly back to ~ 1 (Fig. 5), thus suggesting a possible brief distinct drop in sealevel (Miller *et al.* 2011) associated with enhancement of oxygenation that interrupted the general long-term low oxygen conditions (Landing, 2012, 2013).

Also, Ni was utilized as a proxy of bioproductivity and input of nutrients and terrigenous material (e.g. Śliwiński, Whalen & Day, 2010). Like Th/U

https://doi.org/10.1017/S001675681800002X Published online by Cambridge University Press

values, the Ni contents have very poor correlation with their Sr counterparts ($R^2 < 0.03$; Appendix), thus suggesting insignificant impact by diagenesis. The Ni profile of the investigated carbonate section (Fig. 5) exhibits a short-term fast increase in the water column Ni budget that correlates with the positive Th/U shift, which is consistent with the suggested brief drop in the sealevel that likely resulted in an increase in the input of nutrients and possible enhancement in bioproductivity but for a short time interval.

Both the Th/U and Ni shifts correlate with the peak of the broad negative $\delta^{13}C$ shift on the C-isotope profile of the investigated carbonates (Fig. 5), which also agrees with the suggested brief sealevel drop before it resumed rising again. Although no sealevel profile has been documented for the currently investigated Martin Point section, the sealevel curve, reconstructed from an equivalent but shallow-water section in Utah, USA (Lawson Cove), shows a brief drop at the same stratigraphic level correlated with the base of the *notchpeakensis* Zone (Miller *et al.* 2011, their figure 8). This drop likely resulted in shifting shallower O_2-rich water relatively down to slope settings, which enhanced the oxidation of buried organic matter to release light $^{12}CO_2$ that led to the deposition of ^{13}C-depleted carbonates and caused the negative $\delta^{13}C$ swing. This effect seems to have overprinted the increase in primary productivity, particularly in a slope setting where organic productivity is restricted, to some extent, compared with shallow-shelf environments. Also, the low abundance of marine and terrestrial biota during the very early Palaeozoic would argue against significant inputs of weathered light carbon into the ocean. The consistency of evidence from trace elements with that from the C-isotopes suggests that the uppermost Cambrian carbonates of the investigated Martin Point Formation were deposited likely under dysoxic rather than anoxic conditions, which is similar to conditions of the deposition of the Cambrian–Ordovician GSSP sediments at Green Point (e.g. Azmy *et al.* 2014, 2015). Thus, this demonstrates that the stratigraphic level of the peak of the broad negative $\delta^{13}C$ shift represents the well-documented HERB event known for the Late Cambrian (e.g. Ripperdan, Magaritz & Kirschvink, 1993; G. S. Nowlan, unpublished report, 1995; Buggisch, Keller & Lehnert, 2003; Jing *et al.* 2008; Landing, Westrop & Adrain, 2011; Miller *et al.* 2011, 2014; Terfelt, Eriksson & Schmitz, 2014).

6.c. Carbon-isotope stratigraphy

The Late Cambrian through Early Ordovician times are known to be associated with global sealevel changes (e.g. James & Stevens, 1986; Cooper, Nowlan & Williams, 2001; Landing, 2007, 2012, 2013; Landing, Westrop & Miller, 2010) that influenced the abundance of biota and their productivity in oceans and/or the preservation of organic debris in sediments. These changes were accordingly reflected in the global ocean water chemistry, particularly the C-isotope composition of marine carbonates during those time intervals that were characterized by two major negative $\delta^{13}C$ excursions, one correlated with the Upper Cambrian HERB event and the other with the Cambrian–Ordovician boundary (e.g. Ripperdan, Magaritz & Kirschvink, 1993; Chen *et al.* 1995; G. S. Nowlan, unpublished report, 1995; Buggisch, Keller & Lehnert, 2003; Jing *et al.* 2008; Miller *et al.* 2011, 2014; Azmy *et al.* 2014; Terfelt, Eriksson & Schmitz, 2014; Li *et al.* 2017). Similar $\delta^{13}C$ excursions, caused by variations in primary productivity or organic preservation, have been documented in marine environments throughout the Earth's history (e.g. Veizer *et al.* 1999; Halverson *et al.* 2005; Landing, 2013).

Eustatic variations during the Late Cambrian through Early Ordovician influenced the oceanic redox conditions (Cooper, Nowlan & Williams, 2001; Landing, 2013), which impacted the primary productivity. Earlier studies indicate that the Upper Cambrian Martin Point carbonates were deposited in a slope setting (James & Stevens, 1986) likely under dysoxic conditions (Azmy *et al.* 2015).

The petrographic and geochemical characteristics of the investigated Martin Point carbonates argue for an insignificant degree of alteration and a high degree of preservation of chemical signatures. This suggests that they retain at least their near-primary $\delta^{13}C$ signatures, particularly when diagenetic fluids do not have much CO_2 that would reset the C-isotope composition of those carbonates. Thus, a reliable chemostratigraphic $\delta^{13}C$ profile can be reconstructed to investigate temporal variations in seawater chemistry during the Late Cambrian.

The $\delta^{13}C$ profile of the currently investigated succession at Martin Point (Fig. 6) exhibits a lower broad C-isotope excursion that ends barely below the stratigraphic level of the boundary between the Martin Point and Broom Point members where an upper excursion occurs. No physical stratigraphic hiatuses have been documented throughout the section (cf. James & Stevens, 1986; Barnes, 1988). The broad excursion (~3 ‰) consists of approximately five main subpeaks (each about 2 ‰) and reaches its maximum at Sample MH7 (Fig. 6). The upper excursion (~2.5 ‰) consists of two main distinctive narrow and sharp subpeaks that match those immediately above the geochemical anomaly level documented by Azmy *et al.* (2014, 2015) at Green Point, and therefore the base of the upper excursion (Fig. 6, Sample MP15) can be reliably correlated with the level of the geochemical anomaly (Azmy *et al.* 2015). The geochemical anomaly level marks distinct changes in the $\delta^{13}C_{org}$, $\delta^{15}N$ and $\delta^{238}U$ profiles of carbonates across the Cambrian–Ordovician GSSP boundary section at Green Point (Azmy *et al.* 2014, 2015) that reflect an increase in dysoxic conditions. The lower broad excursion of the Martin Point C-isotope profile reaches its maximum swing at a subpeak near the bottom of Bed 7 that can be correlated with the HERB (Fig. 6) subpeak documented by Miller *et al.* (2014). The peak value of the negative HERB $\delta^{13}C$ excursion nearly coincides with the lower

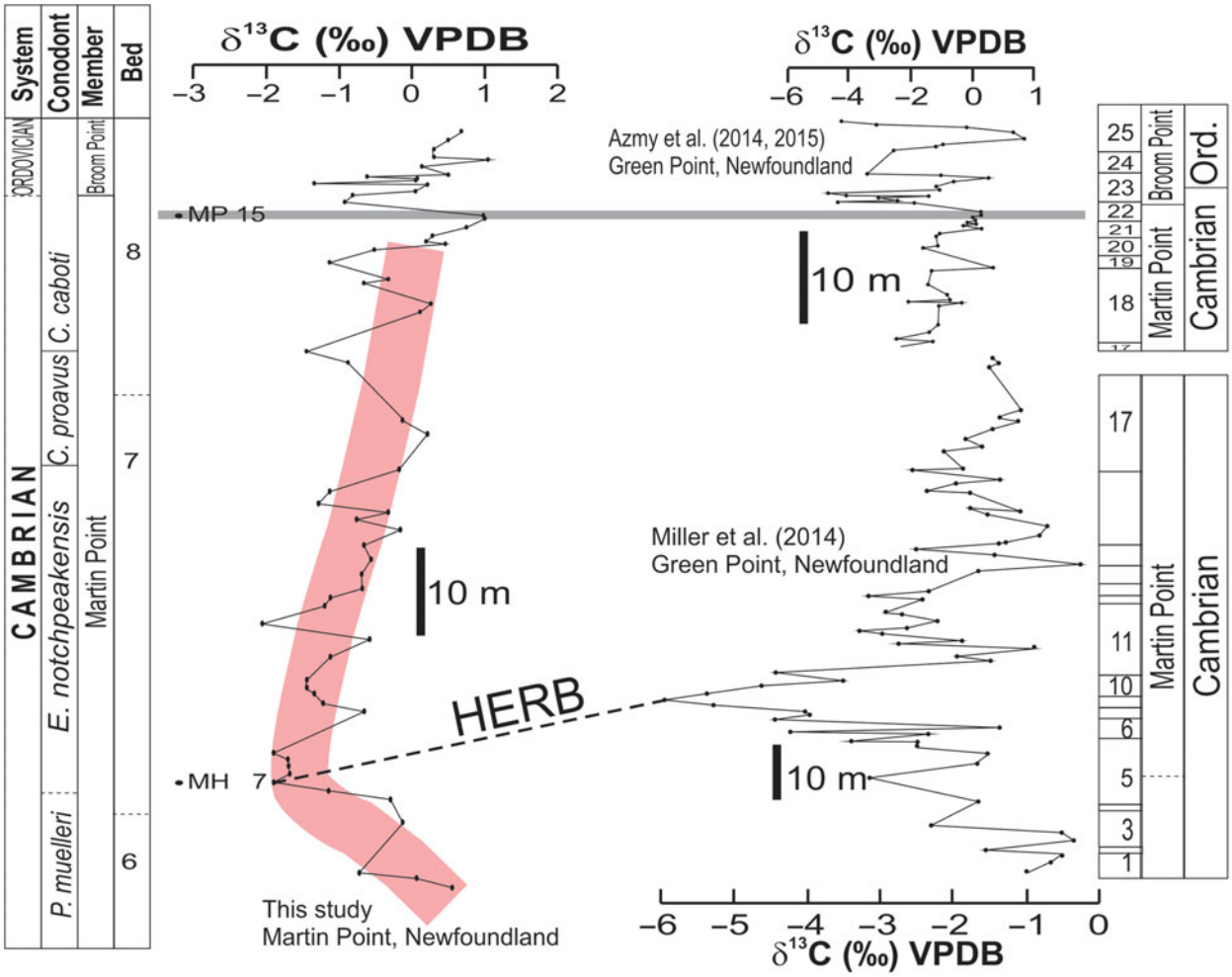

Figure 6. (Colour online) Carbon-isotope profiles spanning the uppermost Cambrian and lowermost Ordovician at Martin Point, Newfoundland (current study), and the uppermost Cambrian (from Miller *et al*. 2011) and the GSSP Cambrian–Ordovician boundary (from Azmy *et al*. 2014) at Green Point in western Newfoundland, Canada. The solid grey line refers to the level of the geochemical anomaly documented by Azmy *et al*. (2014, 2015), and the thick red line shows the general first-order trend of the HERB C-isotope profile of the investigated section at Martin Point.

boundary of the *E. notchpeakensis* biozone (Stouge, Bagnoli & Azmy, 2016), which is the same stratigraphic level of the HERB event documented by earlier studies (Miller *et al.* 2011, 2014) in the equivalent section of Green Point.

The amplitudes of the $\delta^{13}C$ subpeaks and the magnitude of the entire excursion are influenced by the response of organic productivity to changes in sealevel, which varies from basin to basin and from one location to another inside the same basin depending on the position of the investigated sections relative to the palaeogeography (basin depth). The uppermost Cambrian sedimentary rocks in allochthonous western Newfoundland were deposited in a slope setting (James & Stevens, 1986) of restricted light due to depth where dysoxic conditions likely dominated and changes in sealevel would enhance the negative $\delta^{13}C$ shifts on the isotope profile (Azmy *et al.* 2015). Thus, the more negative values and sharper and higher magnitudes of negative $\delta^{13}C$ excursions of the Upper Cambrian – Lower Ordovician carbonates at the Green Point section (Miller *et al.* 2014) relative to their Martin Point counterparts suggest that the Martin Point section was located at relatively shallower level on the slope settings near the boundary of the photic zone where the primary productivity is relatively higher (more positive $\delta^{13}C$), which is also consistent with the thicker sediments of the Martin Point section relative to their equivalent Green Point counterpart (James & Stevens, 1986; Playton, Janson & Kerans, 2010). Unfortunately, no detailed trace element compositions have yet been documented for the Green Point carbonates to allow comparison with those of the current study to shed light on the variations of dysoxic conditions.

The negative $\delta^{13}C$ excursions of the Upper Cambrian carbonates at Martin Point are not only correlated with their counterparts of the GSSP section at Green Point in western Newfoundland but can also be correlated with other global equivalent excursions spanning the same time interval (Fig. 7) but from shallow-water carbonates (cf. Chen *et al.* 1995; Jing *et al.* 2008; Landing, Westrop & Adrain, 2011; Miller *et al.* 2011, 2014; Azmy *et al.* 2014; Terfelt, Eriksson & Schmitz, 2014, fig. 9; Li *et al.* 2017, fig. 4).

https://doi.org/10.1017/S001675681800002X Published online by Cambridge University Press

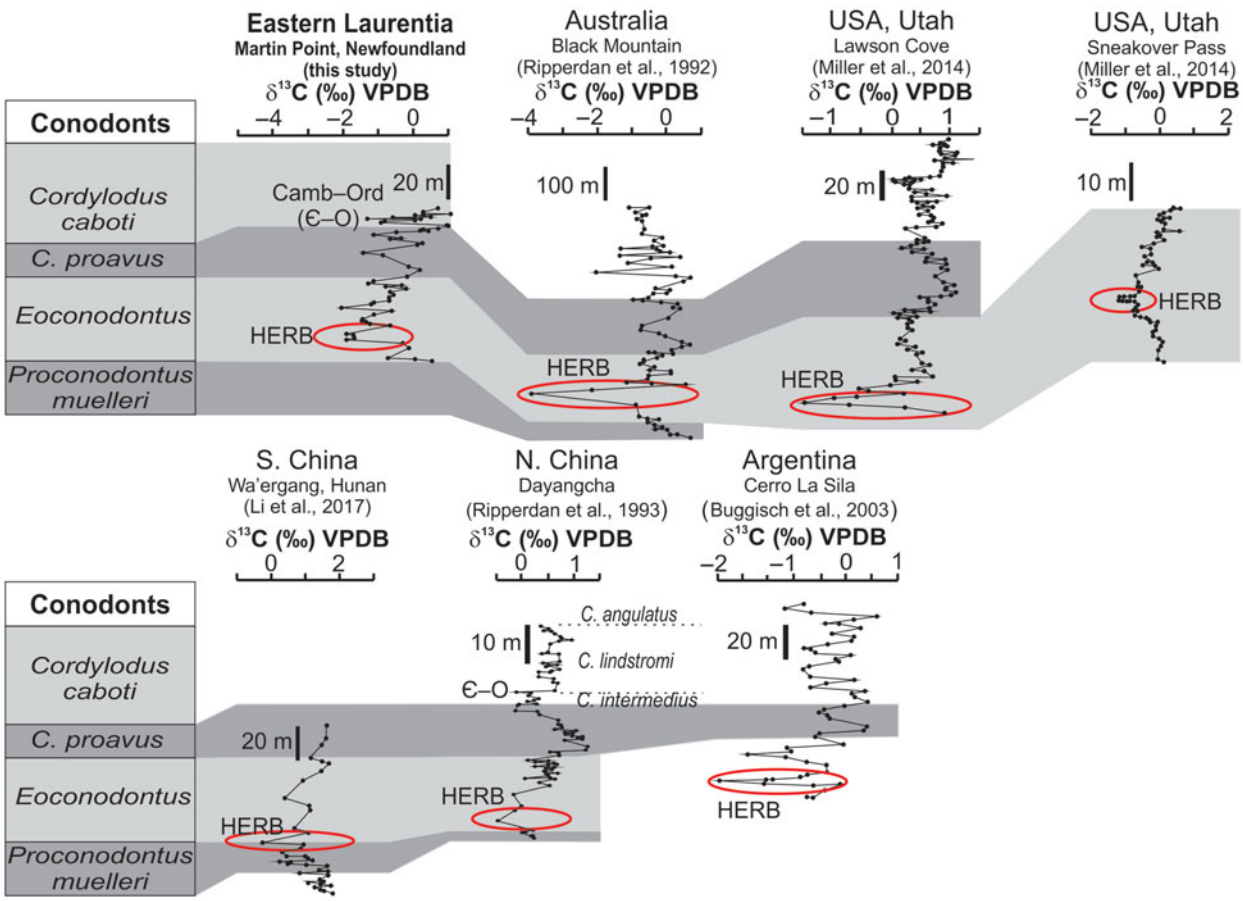

Figure 7. (Colour online) Global carbon-isotope chemostratigraphic correlations of the HERB event (latest Cambrian) documented in sections from basins on different palaeocontinents (modified from Barnes, 1988; Terfelt, Eriksson & Schmitz, 2014; Li *et al.* 2017). The peaks of the $\delta^{13}C$ excursions are marked.

The HERB $\delta^{13}C$ excursion was documented in Utah (Lawson Cove, Sneakover Pass, and Sevier Lake Corral; Miller *et al.* 2011, 2014), Australia (Black Mountain; Ripperdan *et al.* 1992), China (Ripperdan, Magaritz & Kirschvink, 1993; Chen *et al.* 1995; Jing *et al.* 2008; Terfelt, Eriksson & Schmitz, 2014; Li *et al.* 2017) and Argentina (Buggisch, Keller & Lehnert, 2003; Sial *et al.* 2008).

Although earlier investigations (e.g. Glumac & Mutti, 2007) studied the C-isotope profile of the Late Cambrian of northern Appalachia (US), they documented only the older SPICE (Steptoean Positive Carbon Isotope Excursion) event rather than the HERB.

7. Conclusions

- The petrographic and geochemical examinations support the preservation of very near-primary $\delta^{13}C$ signatures in the investigated lime mudstone beds of the continuous Upper Cambrian – Lower Ordovician section at Martin Point in western Newfoundland. The $\delta^{13}C$ profile exhibits two main negative excursions, a lower broad excursion (~3 ‰) that has five subpeaks and reaches its maximum near the base of Bed 7 but ends barely below the stratigraphic level of the boundary between the Martin Point and Broom Point members and an upper narrow excursion (~2.5 ‰) that has two sharp subpeaks immediately above the earlier-documented geochemical anomaly level.
- The lower negative $\delta^{13}C$ excursion is associated with positive shifts on the Th/U and Ni profiles and can also be correlated with the global Late Cambrian HERB event, whereas the upper excursion matches that of the Cambrian–Ordovician GSSP boundary section at Green Point.
- The amplitudes of the major negative excursions of the Martin Point C-isotope profiles are less than those of their Green Point counterparts, which can likely be attributed to the location of the sections within the basin. It is possible that the Martin Point section was located at a relatively shallower setting where the impact of bioproductivity is higher.
- The occurrence of the peak of HERB $\delta^{13}C$ excursion at the base of the *E. notchpeakensis* is a potential tool for the global correlation of the uppermost Cambrian in eastern Laurentia with equivalent sections on the same palaeocontinent and also on others.

Acknowledgements. The author wishes to thank Dr Denis Lavoie and other anonymous reviewers for their constructive reviews. Also, the efforts of Dr Chad Deering (editor) are much appreciated. Special thanks to Dr Svend Stouge for his help in the field. This project was supported by funding (to

Karem Azmy) from the Petroleum Exploration Enhancement Program (PEEP), NL, Canada.

References

Arnaboldi, M. & Meyers, P. A. 2007. Trace element indicators of increased primary production and decreased water-column ventilation during deposition of latest Pliocene sapropels at five locations across the Mediterranean Sea. *Palaeogeography, Palaeoclimatology, Palaeoecology* **249**, 425–43.

Azmy, K., Kaufman, A. J., Misi, A. & Oliveira, T. F. 2006. Isotope stratigraphy of the Lapa Formation, São Francisco Basin, Brazil: implications for Late Neoproterozoic glacial events in South America. *Precambrian Research* **149**, 231–48.

Azmy, K., Kendall, K., Brand, U., Stouge, S. & Gordon, G. W. 2015. Redox conditions across the Cambrian-Ordovician boundary: elemental and isotopic signatures retained in the GSSP carbonates. *Palaeogeography, Palaeoclimatology, Palaeoecology* **440**, 440–54.

Azmy, K., Stouge, S., Brand, U., Bagnoli, G. & Riiperdan, R. 2014. High-resolution chemostratigraphy of the Cambrian–Ordovician GSSP in western Newfoundland, Canada: enhanced global correlation tool. *Palaeogeography, Palaeoclimatology, Palaeoecology* **409**, 135–44.

Azmy, K., Veizer, J., Misi, R., De Olivia, T., Sanches, A. L. & Dardenne, M. 2001. Isotope stratigraphy of the Neoproterozoic carbonate of Vazante Formation Saõ Francisco Basin, Brazil. *Precambrian Research* **112**, 303–29.

Azomani, E., Azmy, K., Blamey, N., Brand, U. & Al-Aasm, I. 2013. Origin of Lower Ordovician dolomites in eastern Laurentia: controls on porosity and implications from geochemistry. *Marine and Petroleum Geology* **40**, 99–114.

Bahamonde, J. R., Merino-Tomé, O. A. & Heredia, N. 2007. A Pennsylvanian microbial boundstone-dominated carbonate shelf in a distal foreland margin (Picos de Europa Province, NW Spain). *Sedimentary Geology* **198**, 167–93.

Banner, J. L. & Hanson, G. N. 1990. Calculation of simultaneous isotopic and trace element variations during water-rock interaction with applications to carbonate diagenesis. *Geochimica et Cosmochimica Acta* **54**(11), 3123–37.

Barnes, C. R. 1988. The proposed Cambrian–Ordovician global boundary stratotype and point (GSSP) in western Newfoundland, Canada. *Geological Magazine* **125**, 381–414.

Bartley, J. K., Kah, L. C., Frank, T. D. & Lyons, T. W. 2015. Deep-water microbialites of the Mesoproterozoic Dismal Lakes Group: microbial growth, lithification, and implications for coniform stromatolites. *Geobiology* **13**, 15–32.

Brand, U., Logan, A., Bitner, M. A., Griesshaber, E., Azmy, K. & Buhl, D. 2011. What is the ideal proxy of Paleozoic seawater? *Memoirs of the Association of Australasian Palaeontologists* **41**, 9–24.

Buggisch, W., Keller, M. & Lehnert, O. 2003. Carbon isotope record of Late Cambrian to Early Ordovician carbonates of the Argentine Precordillera. *Palaeogeography, Palaeoclimatology, Palaeoecology* **195**, 357–73.

Cawood, P. A., McCausland, P. J. A. & Dunning, G. R. 2001. Opening Iapetus: constraints from Laurentian margin in Newfoundland. *Geological Society of America Bulletin* **113**, 443–53.

Chen, J., Zhang, J., Nicoll, R. S. & Nowlan, G. S. 1995. Carbon and oxygen isotopes in carbonate rocks within Cambrian–Ordovician boundary interval at Dayangcha, China. *Acta Palaeontologica Sinica* **34**, 393–408.

Coniglio, M. & James, N. P. 1990. Origin of fine-grained carbonate and siliciclastic sediments in an Early Paleozoic slope sequence, Cow Head Group, Western Newfoundland. *Sedimentology* **37**, 215–30.

Cooper, R. A., Nowlan, G. S. & Williams, S. H. 2001. Global Stratotype Section and Point for base of the Ordovician System. *Episodes* **24**, 19–28.

Della Porta, G., Kenter, J. A. M., Bahamonde, J. R., Immenhauser, A. & Villa, E. 2003. Microbial boundstone dominated carbonate slopes (Upper Carboniferous, N. Spain): microfacies, lithofacies distribution and stratal geometry. *Facies* **49**, 175–207.

Derry, L. A., Kaufman, A. J. & Jacobsen, S. B. 1992. Sedimentary cycles and environmental change in the Late Proterozoic: evidence from stable and radiogenic isotopes. *Geochimica et Cosmochimica Acta* **56**, 1317–29.

Dickson, J. A. D. 1966. Carbonate identification and genesis as revealed by staining. *Journal of Sedimentary Petrology* **36**, 491–505.

George, A. D. 1999. Deep-water stromatolites, Canning Basin, Northwestern Australia. *Palaios* **14**, 493–505.

Glumac, B. & Mutti, L. E. 2007. Late Cambrian (Steptoean) sedimentation and responses to sea-level change along the northeastern Laurentian margin: insights from carbon isotope stratigraphy. *Geological Society of America Bulletin* **119**, 623–36.

Halverson, G. P., Hoffman, P. F., Schrag, D. P., Maloof, A. C. & Rice, A. H. N. 2005. Toward a Neoproterozoic composite carbon-isotope record. *Geological Society of America Bulletin* **117**, 1181–207.

Hibbard, J. P., Van Staal, C. R. & Rankin, D. W. 2007. A comparative analysis of pre-Silurian crustal building blocks of the northern and southern Appalachian Orogen. *American Journal of Science* **307**, 23–45.

James, N. P. & Stevens, P. K. 1986. Stratigraphy and correlation of the Cambro–Ordovician Cow Head Group, western Newfoundland. *Geological Survey of Canada Bulletin* **366**, 143 pp.

James, N. P., Stevens, R. K., Barnes, C. R. & Knight, I. 1989. Evolution of a Lower Paleozoic continental-margin carbonate platform, northern Canadian Appalachians. In *Controls on Carbonate Platform and Basin Development* (eds P. D. Crevello, J. L. Wilson, J. F. Sarg & J. F. Read), pp. 123–46. Society of Economic Paleontologists and Mineralogists, Special Publication no. 44.

Jing, X-C, Deng, S-H, Zhao, Z-J, Lu, Y-Z. & Zhang, S-B. 2008. Carbon isotope composition and correlation across the Cambrian–Ordovician boundary in Kalpin Region of the Tarim Basin, China. *Science in China: Earth Sciences* **51**, 1317–59.

Landing, E. 2007. Ediacaran–Ordovician of east Laurentia – geologic setting and controls on deposition along the New York Promontory. In *Ediacaran–Ordovician of East Laurentia: S. W. Ford Memorial Volume* (ed. E. Landing), pp. 5–24. New York State Museum Bulletin 510.

Landing, E. 2012. Time-specific black mudstones and global hyperwarming on the Cambrian–Ordovician slope and shelf of the Laurentia palaeocontinent. *Palaeogeography, Palaeoclimatology, Palaeoecology* **367–368**, 256–72.

Landing, E. 2013. The Great American Carbonate Bank in northeast Laurentia: its births, deaths, and linkage to continental slope oxygenation (Early Cambrian–Late Ordovician). In *The Great American Carbonate Bank, Essays in Honor of James Lee Wilson* (eds J. R. Derby, R. D. Fritz, S. A. Longacre, W. A. Morgan & C. A. Sternbach), 451–92. American Association of Petroleum Geologists Bulletin, Memoir 98.

Landing, E., Westrop, S. R. & Adrain, J. M. 2011. The Lawsonian Stage – the *Eoconodontus notchpeakensis* (Miller, 1969) FAD and HERB carbon isotope excursion define a globally correlatable terminal Cambrian stage. *Bulletin of Geosciences* **86**(3), 621–40.

Landing, E., Westrop, S. R. & Miller, J. F. 2010. Globally practical base for the uppermost Cambrian (Stage 10): FAD of the conodont *Eoconodontus notchpeakensis* and the Housian [sic, read 'Lawsonian' as the abstract text] Stage. In *The 15th Field Conference of the Cambrian Stage Subdivision Working Group. Abstracts and Excursion Guide, Prague, Czech Republic, and south-eastern Germany* (eds O. Fatka & P. Budil), p. 18. Prague: Czech Geological Survey.

Lavoie, D., Desrochers, A., Dix, G., Knight, I. & Hersi, O. S. 2012. The great carbonate Bank in eastern Canada: an overview. In *The Great American Carbonate Bank: The Geology and Economic Resources of Cambrian–Ordovician Sauk Megasequence of Laurentia* (eds J. Derby, R. Fritz, S. Longcare, W. Morgan & C. Sternbach), pp. 499–524. American Association of Petroleum Geologists, Memoir 98.

Li, X., Jenkyns, H. C., Wang, C., Hu, X., Chen, X., Wei, Y., Huang, Y. & Cui, J. 2006. Upper Cretaceous carbon- and oxygen-isotope stratigraphy of hemipelagic carbonate facies from southern Tibet, China. *Journal of Geological Society of London* **163**, 375–82.

Li, D., Zhang, X., Chen, K., Zhang, G., Chen, X., Huang, W., Peng, S. & Shen, Y. 2017. High-resolution C-isotope chemostratigraphy of the uppermost Cambrian stage (Stage 10) in South China: implications for defining the base of Stage 10 and palaeoenvironmental change. *Geological Magazine* **1**, 1–12.

Machel, H. G. & Burton, E. A. 1991. Factors governing cathodoluminescence in calcite and dolomite, and their implications for studies of carbonate diagenesis. In *Luminescence Microscopy and Spectroscopy, Qualitative and Quantitative Applications* (eds C. A. Barker & O. C. Kopp), pp. 37–57. Society of Economic Paleontologists and Mineralogists (SEPM) Short Course Notes 25.

Miller, J. F., Evans, K. R., Freeman, R. L., Ripperdan, R. L. & Taylor, J. F. 2011. Proposed stratotype for the base of the Lawsonian Stage (Cambrian Stage 10) at the first appearance datum of Econodontus notchpeakensis (Miller) in the house Range, Utah, USA. *Bulletin of Geosciences* **86**, 595–620.

Miller, J. F., Repetski, J. E., Nicoll, R. S., Nowlan, G. & Ethington, R. L. 2014. The conodont Iapetognathus and its value for defining the base of the Ordovician System. *GFF* **136**, 185–8.

Playton, T. E., Janson, X. & Kerans, C. 2010. Carbonate slopes. In *Facies Models 4* (eds N. P. James & R. W. Dalrymple). GEOtext 6. St John's: Geological Association of Canada, 586 pp.

Ripperdan, R. L., Magaritz, M. & Kirschvink, J. L. 1993. Carbon isotope and magnetic polarity evidence for non-depositional events within the Cambrian–Ordovician boundary section at Dayangcha. Jilin Province, China. *Geological Magazine* **130**, 443–52.

Ripperdan, R. L., Magaritz, M., Nicoll, R. S. & Shergold, J. H. 1992. Simultaneous changes in carbon isotopes, sea level, and conodont biozones within the Cambrian-Ordovician boundary interval at Black Mountain, Australia. *Geology* **20**, 1039–41.

Rush, P. F. & Chafetz, H. S. 1990. Fabric retentive, non-luminescent brachiopods as indicators of original $\delta^{13}C$ and $\delta^{18}O$ compositions: a test. *Journal of Sedimentary Petrology* **60**, 968–81.

Sial, A. N., Peralta, S., Gaucher, C., Alonso, R. N. & Pimentel, M. A. 2008. Upper Cambrian carbonate sequences of the Argentine Precordillera and the Steptoean C-isotope positive excursion (SPICE). *Gondwana Research* **13**, 437–52.

Śliwiński, M. G., Whalen, M. T. & Day, J. 2010. Trace element variations in the middle Frasnian *punctata* zone (late Devonian) in the western Canada sedimentary basin – changes in oceanic bioproductivity and paleoredox spurred by a pulse of terrestrial afforestation? *Geologica Belgica* **13**, 459–82.

Stouge, S., Bagnoli, G. & Azmy, K. 2016. The Cambrian HERB excursion (Furongian) from the Martin Point Member of the Cow Head Group, western Newfoundland, Canada. In *Palaeo Down Under 2, Adelaide, July 2016* (eds J. R. Laurie, P. D. Kruse, D. C. Garcia-Bellido & J. D. Holmes), p. 56. Geological Society of Australia Abstracts 117.

Terfelt, F., Eriksson, M. E. & Schmitz, B. 2014. The Cambrian–Ordovician transition in dysoxic facies in Baltica – diverse faunas and carbon isotope anomalies. *Palaeogeography, Palaeoclimatology, Palaeoecology* **394**, 59–73.

Veizer, J. 1983. Chemical diagenesis of carbonates. In *Theory and Application of Trace Element Technique: Stable Isotopes in Sedimentary Geology* (eds M. A. Arthur, T. F. Anderson, I. R. Kaplan, J. Veizer & L. S. Land), pp. III-1–III-100. Society of Economic Paleontologists and Mineralogists (SEPM) Short Course Notes 10.

Veizer, J., Ala, D., Azmy, K., Bruckschen, P., Bruhn, F., Buhl, D., Carden, G., Diener, A., Ebneth, S., Goddris, Y., Jasper, T., Korte, C., Pawellek, F., Podlaha, O. & Strauss, H. 1999. $^{87}Sr/^{86}Sr$, $\delta^{18}O$ and $\delta^{13}C$ evolution of Phanerozoic seawater. *Chemical Geology* **161**, 59–88.

Wignall, P. B. & Twitchett, R. J. 1996. Oceanic anoxia and the end Permian mass extinction. *Science* **272**, 1155–8.

Wignall, P. B., Zonneveld, J.-P., Newton, R. J., Amor, K., Sephton, M. A. & Hartley, S. 2007. The end Triassic mass extinction record of Williston Lake, British Columbia. *Palaeogeography, Palaeoclimatology, Palaeoecology* **253**, 385–406.

Williams, S. H. & Stevens, R. K. 1991. Late Tremadoc graptolites from western Newfoundland. *Palaeontology* **34**, 1–47.

Wilson, J. L., Medlock, P. L., Fritz, R. D., Canter, K. L. & Geesaman, R. G. 1992. A review of Cambro-Ordovician breccias in North America. In *Paleokarst, Karst-Related Diagenesis and Reservoir Development: Examples from Ordovician–Devonian Age Strata of West Texas and Mid-Continent* (eds M. P. Candelaria & C. L. Reed), pp. 19–29. Permian Basin Section, Society of Economic Paleontologists and Mineralogists. SEPM Publication no. 92-33.

Appendix. Elemental and isotopic geochemical compositions of Martin Point carbonates

Sample id #	$\delta^{13}C$ (‰VPDB)	$\delta^{18}O$ (‰VPDB)	$CaCO_3$ (%)	$MgCO_3$ (%)	Mn (ppm)	Sr (ppm)	Ni (ppm)	Th (ppm)	U (ppm)
MH1	0.6	– 7.1	98.5	1.5	150	687	3.1	0.58	0.352
MH2	0.1	– 7.1							
MH3	– 0.7	– 7.1	98.6	1.4	335	536	3.6	0.66	0.408
MH4	– 0.1	– 7.6							
MH5	– 0.3	– 6.9	98.2	1.8	253	980	4.1	0.24	0.194
MH6	– 1.1	– 7.8							
MH7	– 1.9	– 7.6	98.5	1.5	271	596	3.9	0.61	0.223
MH8	– 1.7	– 7.3							
MH9	– 1.7	– 7.6	98.4	1.6	339	498	5.2	0.85	0.219
MH10	– 1.7	– 7.5							
MH11	– 1.9	– 7.8	98.2	1.8	433	233	6.3	2.15	0.426
MH12	– 0.7	– 7.8							
MH13	– 1.2	– 7.8							
MH14	– 1.3	– 7.1							
MH15	– 1.4	– 7.2	97.9	2.1	572	187	5.4	1.19	0.331
MH16	– 1.4	– 7.3							
MH17	– 1.1	– 7.5							
MH18	– 0.6	– 7.3	98.9	1.1	387	216	8.5	0.55	1.980
MH19	– 2.1	– 7.3	97.2	2.8	438	165	3.7	0.88	0.970
MH20	– 1.2	– 7.2							
MH21	– 1.1	– 7.1							
MH22	– 0.7	– 6.9							
MH23	– 0.7	– 7.0							
MH24	– 0.6	– 7.0	98.9	1.1	228	238	2.7	0.39	0.936
MH25	– 0.7	– 7.0							
MH26	– 0.2	– 6.8							
MH27	– 0.8	– 7.1							
MH28	– 0.3	– 7.2							
MH29	– 1.3	– 6.9	98.8	1.2	562	218	2.7	0.43	3.573
MH30	– 1.1	– 7.6							
MH31	– 0.2	– 7.2							
MH32	0.2	– 7.0	98.7	1.3	183	231	2.4	0.23	0.950
MH33	– 0.1	– 6.9							
MP1	– 0.9	– 7.1							
MP2	– 1.5	– 7.0	98.8	1.2	292	310	1.9	0.14	0.824
MP3	0.1	– 6.8							
MP4	0.3	– 6.8							
MP5	0.6	– 6.8	99.0	1.0	523	250	2.1	0.21	1.598
MP6	– 0.7	– 7.1							
MP7	– 0.3	– 6.6							
MP8	– 1.1	– 7.2	97.3	2.7	360	262	3.6	0.58	2.142
MP9	– 0.5	– 6.8							
MP10	0.5	– 6.8	98.9	1.1	569	247	2.3	0.27	0.751
MP11	0.2	– 6.8							
MP12	0.3	– 7.1							
MP13	0.8	– 6.9							
MP14	1.0	– 6.5	99.0	1.0	569	194	7.3	1.49	2.626
MP15	1.0	– 6.4							
MP16	– 0.9	– 6.8	98.7	1.3	649	229	2.0	0.53	1.561
MP17	– 0.8	– 6.5							
MP18	0.1	– 6.8							
MP19	0.2	– 6.5	98.6	1.4	187	291	2.1	0.49	0.797
MP20	– 1.3	– 7.4	96.3	3.7	297	152	3.4		0.387
MP21	0.1	– 7.1							
MP22	0.1	– 7.0	98.3	1.7	142	275	2.9	0.70	1.652
MP23	– 0.6	– 7.0	98.3	1.7	301	301	1.4	0.32	0.626
MP24	0.5	– 6.9							
MP25	0.1	– 7.0							
MP26	1.0	– 6.6	99.0	1.0	169	247	2.0	0.24	0.321
MP27	0.3	– 6.7							
MP28	0.3	– 6.6	98.8	1.2	586	283	2.8	0.24	0.345
MP29	0.5	– 6.7							
MP30	0.7	– 6.6	98.9	1.1	201	284	2.4	0.22	0.828